Static damage surface signatures for laminated plates

P. M. Mohite* and C. S. Upadhyay†

Indian Institute of Technology Kanpur 208016 India

In the present paper continuum damage based meso-model proposed by Ladvèze is used to predict the response of initially damaged laminated composites. The model is based on three foundations of meso-model, internal variable approach and method of local state. The present model is refined by replacing the interface as a very thin layer of resin. Further, this layer uses higher order approximation in transverse direction for displacement field over linear variation used in original model. This model has been implemented in the generalized layerwise and and region-by-region finite element models developed by authors. It is seen that the fibre failure mode is dominant comapared to other failure modes in giving significant difference in transverse displacement signature profiling whereas the delamination mode has weak effect. The in-plane strains also show similar behaviour. Here, the results are presented for different shapes and sizes of damage under the transverse load only.

1. Nomenclature

u, v, w	Generalized displacement field
p_{xy}	Inplane approximation order
p_z^i	Transverse approximation order for i^{th} displacement component
E_D	The strain energy of the damaged ply
E_D^I	The strain energy of the damaged interface
Y_{d_F}, $Y_{d'}$, Y_d	Thermodynamic forces associated with mechanical dissipation in ply
Y_{d_1}, Y_{d_2}, Y_{d_3}	Thermodynamic forces associated with mechanical dissipation in three modes for interface

*Graduate Student, Department of Aerospace Engineering, and Students Member.

†Corresponding author (shekhar@iitk.ac.in) Associate Professor, Department of Aerospace Engineering, and Non Member.

d_F, $d^{'}$, d	Damage parameters for fibre breakage, matrix cracking and fibre matrix debonding, respectively
d_1, d_2, d_3	Damage parameters for inteface in three modes
$\bar{\varepsilon}_{xx}$, $\bar{\varepsilon}_{xy}$, $\bar{\varepsilon}_{yy}$	Non-dimensionalized in-plane stresses.

2. Introduction

Unidirectional fiber-reinforced composites are widely used in aerospace applications. They are used for the critical structural applications. These structures are subjected to complex aerodynamic and service loads. They exhibit progressive failure and hence deterioration of elastic moduli. The mechanics by which failure occurs are numerous. These can be broadly categorized as ply level failure mechanisms like brittle fibre failure, fibre matrix debonding, and matrix cracking; and delamination. A exhaustive literature is available for the initiation of damage in the laminates.

The continuum based damage meso-model is capable of predicting both initiation and growth of damage in these laminates. Further, it is also capable of predicting delamination initiation and its growth. The concept was first introduced by Kachanov[1] for creep damage in metal. This concept is taken by Ladevèze and his co-workers[2-7] and others[8,9] and extended to laminated composites. In the following section, the details of the plate models used in this study and meso-model are presented in brief.

3. Plate Models

Several families of plate models have been proposed in the literature[11-14] for the analysis of homogeneous and laminated plates. These families can be broadly categorized as (a) shear deformable theories (b) zig-zag theories (c) layer-by-layer or three dimensional analysis.

The plate models used in this study are based on generalized forms of the shear deformable theories and layer-by-layer theories. In general, the models proposed in the literature are for bending dominated problems. For such problems it can be shown that the transverse displacement is symmetric (with respect to the depth coordinate z) while the in-plane displacements are antisymmetric. However, this is true only for symmetric laminates. For other cases (e.g. anti-symmetric, unsymmetric laminates and laminates with ply level or delamination damage), the deformation has both bending and membrane components. This requires a general representation of the displacement field (through the thickness). In the following, we outline the plate models which are used in this study.

A. Layerwise Plate Model (LM)

This is the most general three-dimensional representation of the displacement field. The director functions are defined as the one dimensional basis functions over each lamina. From Fig. 1, it can be seen that the representation of the displacement field is given by (see[11,12] for details):

$$\begin{aligned} u(x,y,z) &= \sum_{i=1}^{n_1} u_i(x,y)\,\bar{M}_i(z) \\ v(x,y,z) &= \sum_{i=1}^{n_2} v_i(x,y)\,\bar{M}_i(z) \\ w(x,y,z) &= \sum_{i=1}^{n_3} w_i(x,y)\,\bar{M}_i(z) \end{aligned} \tag{1}$$

where $n_1 = n_2$ and n_3 depend on the order of approximation $p_z^u = p_z^v$, p_z^w and the number of laminae (or layers) nl in the laminate. Hence, here the number of unknowns grows with the number of laminae. Members of this family of models will be represented by $LMp_{xy}p_z^u p_z^v p_z^w$.

B. Region-by-region Plate Model (RR)

The idea of region-by-region modeling approach is to put any model in any region of the domain. In the vicinity of the cut-outs and the outer boundaries of the domain, the solution is expected to be unsmooth, have severe boundary layer effect, and possibly be three-dimensional in nature. Hence along with a refinement of the mesh, enrichment of the model will also be desired in these regions. It was shown in[11]-[13] that layerwise model are very effective in capturing the three dimensional effects at these structural details while elsewhere equivalent single layer models with postprocessed transverse stresses can be used.

The details of implementation of region-by-region model can be seen in.[11,13]

4. Finite Element Formulation

The potential energy, Π, for the structure is given by

$$\Pi = \tfrac{1}{2}\int_V \{\sigma(u)\}^T \{\varepsilon(u)\}\, dV \; - \int_{R^+\cup R^-} T_3\, u_3\, ds - \int_{T_N} (T_1 u_1 + T_2 u_2)\, ds \tag{2}$$

where V is the volume enclosed by the plate domain; $R^+$and $R^-$are the top and bottom faces of the plate $T_3(x,y)$ is the applied transverse load on these faces; Γ are the lateral faces with $\Gamma = \Gamma_N \cup \Gamma_D$ and $\Gamma_N =$ Neumann boundary, $\Gamma_D =$ Dirichlet boundary; T_1, T_2 are the tractions specified on the lateral faces (in-plane loading).

The solution to the problem, $\mathbf{u}_M$, is the minimizer of the total potential, Π, and is obtained from the solution of the following weak problem:

Find $\mathbf{u}_M \in H^\circ$ such that

$$\mathcal{B}(\mathbf{u}_M, \mathbf{v}) = \mathcal{F}(\mathbf{v}) \quad \forall\, \mathbf{v} \in H^\circ \tag{3}$$

where $H^\circ = \{\sigma = |\pi(\mathbf{v}) < \infty \text{ and } \mathbf{M}\,\mathbf{u} = \mathbf{0} \text{ on } \Gamma_D\}$. Further, $\mathcal{B}(\mathbf{u}_M, \mathbf{v}) = \int \sigma(\mathbf{u}_M)\,\varepsilon(\mathbf{v})$

Note that in this study Dirichlet means the part of lateral boundary where geometric constraints are imposed, while Neumann stands for the stress-free parts of the lateral boundary. Further, $\mathbf{M}$ depends on the type of Dirichlet conditions on the edge, i.e. clamped $(u, v, w = 0)$; soft simple-support $(u_n, w = 0)$; hard simple-support $(u_t, w = 0)$ etc. Here, u_n and u_t denotes in-plane displacement normal and tangential to an edge, respectively.

5. Mesomodeling of Laminates

The theory of mesomodeling is based on three foundations as mesoconstituents, method of local state and internal variable approach. The mesomodel is defined by means of two mesoconstituents (see,[2] for example) as individual single layer and interface between two adjacent layers. Each material layer of the laminate is treated as a homogeneous layer in the thickness. The individual layer is reinforced in only one direction. The interface between two adjacent layers is a mechanical surface connecting the adjacent layers and depends on the relative orientation of their fibres. The interface is assumed to be elastic and damageable. The laminate and its meso-constituents are elucidated in Fig. 2. The method of local state relates damage with the thermodynamic forces associated with the strain energy. The internal variables relates the damage through degradation of material's elastic moduli.

A mesomodel is then defined by adding another assumption of a uniform damaged state throughout the thickness of the elementary ply. This assumption plays a major role when trying to simulate crack with a damage model.

6. Single-Layer Modeling

As specified in the beginning of this section, the laminate is modeled as a stacking of elementary constituents. In the elementary ply modeling, the plane stress state is assumed.

A. Damage Kinematics of Ply

The composite materials (e.g. carbon-fibre/epoxy-resin) under consideration in the study have only one reinforced direction (unidirectional fibre composites). The energy of the damaged material defines the damage kinematics.

The unilateral aspect of microcracking is taken into account by splitting the energy into a "tension" energy and a "compression" energy. Thus, the strain energy of the damaged structure is given as

1. *Tension (distortion) energy*: This part of the energy is responsible for initiation and propagation of damage.

2. *Compression energy*: This part of the energy can cause "healing" of damage as the microcracks may coalesce or chemical reactions at the microcrack surfaces may close the gap. The microcracks may close under the effect of compression energy and act like undamaged parts transferring displacement and forces without any loss.

Remark: Although, the compression energy can cause the healing of damage, in the proposed model the state of damage is treated as dormant. That is, under compression energy the state of damage of already damaged region do not reduce and remains constant.

Remark: In general, the classical continuum damage models do not allow for the coupling and interaction between the damaged and undamaged parts. This aspect of modeling of damage has significant consequences, as the effect of neighbouring damaged regions is not included in the characterization. The modeling of the healing effect of damage has been attempted in open literature. One such approach is given as 'disturbed state concept' due to Desai.[10]

In the following, the subscripts 1, 2 and 3 designate the fibre direction, the transverse direction inside the layer and the normal direction, respectively. The strain energy of the damaged ply is given as[2]

$$\begin{aligned} E_D = \frac{1}{2(1-d_F)} \Bigg[& \frac{\langle \sigma_{11} \rangle_+^2}{E_{11}^0} + \frac{\phi \langle \sigma_{11} \rangle_-}{E_{11}^0} - \left(\frac{\nu_{21}^0}{E_{22}^0} + \frac{\nu_{12}^0}{E_{11}^0} \right) \sigma_{11} \sigma_{22} - \left(\frac{\nu_{31}^0}{E_{33}^0} + \frac{\nu_{13}^0}{E_{11}^0} \right) \sigma_{11} \sigma_{33} \\ & - \left(\frac{\nu_{32}^0}{E_{33}^0} + \frac{\nu_{23}^0}{E_{22}^0} \right) \sigma_{22} \sigma_{33} \Bigg] + \frac{\langle \sigma_{22} \rangle_-^2}{E_{22}^0} + \frac{\langle \sigma_{33} \rangle_-^2}{E_{33}^0} \\ & + \frac{1}{2} \left[\frac{1}{(1-d')} \left(\frac{\langle \sigma_{22} \rangle_+^2}{E_{22}^0} + \frac{\langle \sigma_{33} \rangle_+^2}{E_{33}^0} \right) + \frac{1}{(1-d)} \left(\frac{\sigma_{12}^2}{G_{12}^0} + \frac{\sigma_{23}^2}{G_{23}^0} + \frac{\sigma_{31}^2}{G_{31}^0} \right) \right] \end{aligned} \tag{4}$$

where $\langle \cdot \rangle_+$ and $\langle \cdot \rangle_-$ denote the positive and negative parts of quantity in parenthesis, respectively. The superscript 0 denotes the virgin or undamaged quantity. d_F, d' and d are three scaler internal variables which

remain constant within the thickness of each single-layer and serve to describe the damage mechanisms inside the ply. The variable d_F characterizes the damage of the fibre, d' characterizes the matrix cracking and d characterizes the fibre matrix interfacial debonding damage. ϕ is a material function which takes into account the non-linear response in compression. The material function is defined such that $\frac{\partial^2 E_D}{\partial^2 \sigma_{11}} = \frac{1}{E^c_{11}}$.

The non-linear compressive behaviour is modeled by degrading the Young's modulus of the fibre, E^0_{11} in.[2, 4, 5, 7] The main result is that the behaviour is purely elastic but non-linear. The compression modulus E^c_{11} can be written as (see[6, 7] and references therein)

$$E^c_{11} = E^0_{11}\left[1 - \tfrac{\alpha}{E^0_{11}}\langle\sigma_{11}\rangle_-\right]$$

where α is a material constant.

Remark: Here, it is to be noted that in the present model the tensile behaviour of the fibres is characterized. The compressive behaviour of the fibres is not taken into account.

The thermodynamic forces associated with the mechanical dissipation are

$$\begin{aligned}
Y_{d_F} &\equiv \tfrac{\partial}{\partial d_F}\langle\langle E_D\rangle\rangle_{|\sigma=\text{const.}} = \tfrac{1}{2(1-d_F)^2}\left\langle\left\langle \tfrac{\langle\sigma_{11}\rangle_+^2}{E^0_{11}} + \tfrac{\phi\langle\sigma_{11}\rangle_-}{E^c_{11}} - \left(\tfrac{\nu^0_{21}}{E^0_{22}} + \tfrac{\nu^0_{12}}{E^0_{11}}\right)\sigma_{11}\sigma_{22}\right.\right. \\
&\qquad\left.\left. - \left(\tfrac{\nu^0_{31}}{E^0_{33}} + \tfrac{\nu^0_{13}}{E^0_{11}}\right)\sigma_{11}\sigma_{33} - \left(\tfrac{\nu^0_{32}}{E^0_{33}} + \tfrac{\nu^0_{23}}{E^0_{22}}\right)\sigma_{22}\sigma_{33}\right\rangle\right\rangle \\
Y_{d'} &\equiv \tfrac{\partial}{\partial d'}\langle\langle E_D\rangle\rangle_{|\sigma=\text{const.}} = \tfrac{1}{2(1-d')^2}\left\langle\left\langle \tfrac{\langle\sigma_{22}\rangle_+^2}{E^0_{22}} + \tfrac{\langle\sigma_{33}\rangle_+^2}{E^0_{33}}\right\rangle\right\rangle \\
Y_d &\equiv \tfrac{\partial}{\partial d}\langle\langle E_D\rangle\rangle_{|\sigma=\text{const.}} = \tfrac{1}{2(1-d)^2}\left\langle\left\langle \tfrac{\sigma_{12}^2}{G^0_{12}} + \tfrac{\sigma_{23}^2}{G^0_{23}} + \tfrac{\sigma_{31}^2}{G^0_{31}}\right\rangle\right\rangle
\end{aligned} \tag{5}$$

where the symbol $\langle\langle\cdot\rangle\rangle$ indicates that the value is averaged through the thickness of the layer. This represents the key assumption of the meso-model, that the damage state is uniform through the thickness of each meso-constituent. The proposed model is given in.[2]

Remark: In the present finite element implementation, the damage is assumed to be constant in the entire volume of an element.

7. Interlaminar Interface Model

A. Damage Kinematics of the Interface

Following,[2],[8] the interlaminar connection is modeled as a two-dimensional entity which ensures stress and displacement transfers from one ply to another. The interlaminar connection can be classically interpreted

as a ply of matrix material. The thickness (denoted by e) is small compared to the in-plane dimensions. As shown in Fig. 3, the principal directions 1, 2 and 3 of the interface are described in terms of the bisector of the angle θ between the fibre orientations of the adjoining layers. It is assumed that the bisectors (N_1 and N_2) of the angle formed by the fibre directions of the adjacent plies are orthotropic directions. The interface material model is developed following the same approach used for deriving the single-layer model. The displacement discontinuity at the interface can be represented as

$$\mathbf{u} = \mathbf{u}^+ - \mathbf{u}^- = u_1 N_1 + u_2 N_2 + u_3 N_3 \tag{6}$$

where $\mathbf{u}^+$ is displacement field of the bottom face of the upper layer and $\mathbf{u}^-$ is that of the top face of the lower layer. In the global co-ordinate x, y and z directions these are given as $\mathbf{u}^+ = \left\{u_x^+ \; u_y^+ \; u_z^+\right\}^T$ and $\mathbf{u}^- = \left\{u_x^- \; u_y^- \; u_z^-\right\}^T$. The displacement discontinuity between the bottom face of the top layer and top face of the bottom layer can be given as

$$\mathbf{u} = \left\{ \begin{array}{c} u_1 \\ u_2 \\ u_3 \end{array} \right\} = \left\{ \begin{array}{c} (u_x^+ - u_x^-)\, cos\theta - \left(u_y^+ - u_y^-\right) sin\theta \\ (u_x^+ - u_x^-)\, cos\theta + \left(u_y^+ - u_y^-\right) sin\theta \\ u_z^+ - u_z^- \end{array} \right\} \tag{7}$$

It is then possible to use $\mathbf{u}$ in the formulation of a strain-displacement relationship for the interface if the assumption is made that gradients within the 12 plane are very small compared to those in the 13 and 23 planes. The out-of-plane strain components ε_{33}, ε_{31} and ε_{32} can be defined solely by the through-the-thickness gradients. These can be approximated as

$$\begin{aligned} \varepsilon_{33} &= \tfrac{\partial u_3}{\partial x_3} \approx \tfrac{u_3}{e} \\ 2\varepsilon_{31} &= \tfrac{\partial u_1}{\partial x_3} + \tfrac{\partial u_3}{\partial x_1} \approx \tfrac{\partial u_1}{\partial x_3} \approx \tfrac{u_1}{e} \\ 2\varepsilon_{32} &= \tfrac{\partial u_2}{\partial x_3} + \tfrac{\partial u_3}{\partial x_2} \approx \tfrac{\partial u_2}{\partial x_3} \approx \tfrac{u_2}{e} \end{aligned} \tag{8}$$

defining elastic constants of the interface k_{33}, k_{31} and k_{32} as

$$\begin{aligned} k_{33} &= \tfrac{E_{33}}{e} \\ k_{31} &= \tfrac{2G_{13}}{e} \\ k_{32} &= \tfrac{2G_{23}}{e} \end{aligned} \tag{9}$$

Remark: The value of the interface thickness is generally taken as $e \approx \frac{1}{10} t_{min}$, where t_{min} is minimum of thickness of adjacent plies. The thickness is of the order of 0.01 mm or two fibre diameters (see[9]).

Remark: In the present implementation, the fictitious interfacial layer is replaced by the actual isotropic matrix layer. For the solution, the interface is also considered as a separate material layer. This leads to a better representation of the local stress state in the interfacial layer.

A constitutive relation that relates the displacement discontinuities between the two adjacent layers to the interlaminar stresses of the interface is introduced as

$$\left\{ \begin{array}{c} \sigma_{31} \\ \sigma_{32} \\ \sigma_{33} \end{array} \right\} = \left[\begin{array}{ccc} k_{31}\left(1-d_1\right) & 0 & 0 \\ 0 & k_{32}\left(1-d_2\right) & 0 \\ 0 & 0 & k_{33}\left(1-d_3\right) \end{array} \right] \left\{ \begin{array}{c} u_1 \\ u_2 \\ u_3 \end{array} \right\} \tag{10}$$

where the subscripts of the internal damage variables d_3, d_1, and d_2 correspond to the associated three fracture mechanics delamination modes (mode I, II and III, respectively). The delamination modes are shown in Fig. 4. The damage of the interlaminar interface is dominated by the transverse stress components. Hence, using transverse stresses, in a form analogous to that of the layer, the damaged strain energy (per unit area) of the interface is given as

$$E_D^I = \frac{1}{2}\left[\frac{\langle \sigma_{33} \rangle_-^2}{k_{33}} + \frac{\langle \sigma_{33} \rangle_+^2}{k_{33}\left(1-d_3\right)^2} + \frac{\sigma_{32}^2}{k_{32}\left(1-d_2\right)} + \frac{\sigma_{31}^2}{k_{31}\left(1-d_1\right)} \right] \tag{11}$$

Differentiation of Eq. (11) with respect to each damage variable yields the following associated thermodynamic forces, associated with the dissipated energy ω, for each of the three considered delamination modes.

$$Y_{d_3} \equiv \tfrac{1}{2} \tfrac{\langle \sigma_{33} \rangle_+^2}{E_{33}^0 (1-d_3)^2}; \quad Y_{d_1} \equiv \tfrac{1}{2} \tfrac{\sigma_{31}^2}{G_{13}^0 (1-d_1)^2}; \quad Y_{d_2} \equiv \tfrac{1}{2} \tfrac{\sigma_{32}^2}{G_{23}^0 (1-d_2)^2} \tag{12}$$

As with the layer definition, the contribution to the damaged strain energy from normal stress components is separated into tensile and compressive term in order to distinguish between the mechanical effects of a crack opening versus that of crack closing.

Remark: In the present study, the displacement field of the interface is approximated (with higher order) as that of the layer. Hence, the strain energy of the interface, instead of Eq. (11), can be given as

$$E_D^I = \frac{1}{2}\left[\frac{\langle\sigma_{33}\rangle_-^2}{E_{33}} + \frac{\langle\sigma_{33}\rangle_+^2}{E_{33}\left(1-d_3\right)^2} + \frac{\sigma_{32}^2}{G_{23}\left(1-d_2\right)} + \frac{\sigma_{31}^2}{G_{13}\left(1-d_1\right)}\right] \tag{13}$$

Remark: For numerical examples, the damage in a ply is denoted by three damage scalars as $\left(d_F,\, d^{'},\, d\right)$ and in an interface as $(d_1,\, d_2,\, d_3)$.

8. Static Damage Surface Signatures

In this section the effect of preexisting embedded static damage in $M55J/M18$ high modulus Graphite/Epoxy composite material is studied through the transverse deflections and in-plane strain components at the top surface (damage signatures) of the laminate. The material properties are given in Table 1. Here, a [0/90/0] square laminate with all edges hard simple support under a uniformly distributed load of $0.005\,N/mm^2$ is considered. The thickness of each ply is $0.1\,mm$. Further, geometrically graded sublayers (with grading factor $q = 0.15$) are used in the 0° layers, with the grading done towards the interface with the 90° layer. The interfaces between the 0° and 90° layers are taken as $M18$ epoxy layer of $0.01\,mm$ thickness. The plate dimensions are $a = b = 64\,mm$, $(S = 200)$. The properties of $M18$ epoxy are given in Table 2. The damage parameters for ply and interface are given in Table 3.

The maximum in-plane strain component on the top of the laminate is used as quantity of interest for the discretization error control using focussed adaptivity. The specified tolerance for discretization error control was $\eta_1 = \eta_2 = 5\%$. In the region $15 \leq x,\, y \leq 50$ $LM3333$ model is used while in the remaining domain $EQ3333$ model is used.

The transverse deflection and in-plane strain components on the top of the laminate are plotted along the lines $x = \frac{a}{2}$ and $y = \frac{b}{2}$, as given in Fig. 7-17. The strain components are normalized by the maximum value of the strain ε_{xx} obtained for the virgin laminate, in order to see the effect of the damage.

The effect of size of damage on the damage signature is studied for different levels of damage in a ply (see Fig. 7-11) and interface (see Fig. 12 and 13). Damage of two sizes, $10.7 \times 10.7\,mm^2$ (*size1*) and $5.35 \times 5.35\,mm^2$ (*size2*), at the centre of laminate are studied. Further, the effect of shape of damage for different levels of damage in a ply (see Fig. 14-16) and an interface (see Fig. 17) is studied. Damage of square shape with size *size1* and circular shape with same area as that of square shape are considered.

From the figures for the transverse deflection it is observed that:

1. As the size of the damage increases the maximum transverse deflection at the centre of the laminate

(where the damage is located) increases. This is because the damage reduces the stiffness.

2. The transverse deflection change is more for damage in the fibres. This is because their contribution to the stiffness is more than that for the matrix.

3. The location of damaged layer in the laminate plays significant role. The damaged layers at the bottom show maximum transverse deflection. Also, the mode of damage plays an important role.

4. In this case, the size and intensity of damage in the interface layer does not have any effect on the displacement. This is because the stiffness contribution of the thin interface is negligible, and for a partially damaged interface, effective load transfer between adjoining layers is still possible.

5. The transverse deflection on the surface shows a distinct change in profile at the projected boundaries of the embedded damaged regions. This is important to sense the existence of internal damage, using a surface deformation profiling.

6. The shape of the damaged region plays an important role. For the circular shape the value of the maximum transverse deflection is slightly larger than that for the square shape (when the damage is in the bottom layer). This is because the circular shape cuts more fibres than the square shape which reduces the stiffness significantly. This is obvious from the strain informations. The surface strain is more sensitive to a square shaped damage. This can be exploited to find out information about possible location, shape and size of damage zones. The effect of shape of damage is not significant for the case of damage in interface.

7. The transverse deflection is insensitive to shape of damage in 90° layer. This is because for the given bending dominated loading and plate configuration, the 0° layers contribute more to stiffness.

8. Although the laminate is symmetric there is no symmetry for transverse displacement and strain components along x and y axes as the damage is not symmetric with respect to the laminate thickness. Also interestingly, when the given static load is applied it can initiate damage at other locations in the same or different laminae (see Fig. 18 and 19 for example) which further destroys the symmetry.

From figures for the in-plane strain components it can be seen that:

1. The normal in-plane strain components $\bar{\varepsilon}_{xx}$ and $\bar{\varepsilon}_{yy}$ are not much sensitive to the size of damage in matrix cracking and fibre matrix debonding mode. The difference in response is because of the

additional damage sites initiated due to static damage present and applied load. Further, in-plane shear strain component $\bar{\varepsilon}_{xy}$ shows significant difference for these modes of damage. Whereas, when the fibre failure damage mode is dominant all the strain component show significant difference. Again, this behaviour is not so significant for this damage mode in 90° layer.

2. The strain components show a distinct change in profile at the projected boundaries of the embedded damaged regions.

3. For damage with larger size the change in profile at the projected boundaries of the embedded damaged regions is significantly larger and distinct than that of smaller size damage.

4. The location of damaged layer in the laminate plays significant role. The damaged layers at the bottom show maximum significantly different strain profiles. For this case, the shear strain component $\bar{\varepsilon}_{xy}$ shows sharp changes at the damage front. This behaviour is sensitive to mode of failure.

5. When the damage is in interface layer the size of the damage does not show much difference in the strain components except due to additional damage sites initiated.

6. With circular shape of the damage the sharp peaks of the strain components seen for square shape damage, in general, are smoothened out.

7. The shape of damage region does not play much role for interfacial damage.

9. Conclusion

A generalized layerwise and region-by-region modeling approach has been used for the analysis of initially damaged laminated composite plates. The continuum based damage mesomodel has been implemented for these models. A detailed study has been carried out damage signatures (transverse deflection and in-plane strains) at top of the laminate for various shapes and sizes of damages. The key points of this study are summarised as follows.

1. The size, shape and intensity of the damage in the ply affects the transverse deflection and in-plane strain components on the top surface of the laminate. As the size and intensity increases the deflection also increases for transverse loading.

2. The size, shape and intensity of damage in interface does not have much effect on transverse deflection and in-plane strain components on the top surface.

3. The symmetry in the response characteristics in the presence of damage is lost.

4. Due to existing damage, new damage sites can be initiated at other locations when a static transverse load is applied.

References

[1]Kachanov, L.M., "Time of the rupture process creep conditions," *Izv. Akad. Nauk SSR Otd Tekh Nauk*, Vol. 8, 1958, pp. 26, 31.

[2]Ladevèze, P., Allix, O., Deü, J. F., and Lévêque, D., "A mesomodel for localisation and damage computation in laminates," *Computer Methods in Appllied Mechanics and Engineering*, Vol. 183, 2000, pp. 105, 122.

[3]Ladevèze, P., and Lubineau, G., "On a damage mesomodel for laminates: micro-meso relationships, possibilities and limits," *Composite Science and Technology*, Vol. 61, 2001, pp. 2149, 2158.

[4]Ladevèze, P., and Lubineau, G., "An enhanced mesomodel for laminates based on micromechanics," *Composite Science and Technology*, Vol. 62, 2002, pp. 533, 541.

[5]Ladevèze, P., and Lubineau, G., "On a damage mesomodel for laminates: micromechanics basis and improvement," *Mechanics of Materials*, Vol. 35(8), 2003 pp. 763, 775.

[6]Ladevèze, P. "A damage computational method for composite structures," *Computers and Structures*, Vol. 44(1/2), 1992, pp. 79, 87.

[7]Allix, O., Ladevèze, P., and Vittecoq, E., "Modeling and identification of the mechanical behaviour of composite laminates in compression," *Composite Science and Technology*, Vol. 51, 1994, pp. 35, 42.

[8]Phillip, E. A., Herakovich, C. T., and Graham, L. L., "Damage development in composites with large stress gradients," *Composite Science and Technology*, Vol. 61, 2001, pp. 2169, 2182.

[9]Allix, O., Lévêque, D., and Perret, L., "Identification and forecast of delamination in composite laminates by an interlaminar interface model," *Composite Science and Technology* Vol. 58, 1998, pp. 641, 678.

[10]Desai, C. S., *Mechanics of Materials and Interfaces. The Disturbed State Concept*, CRC Press, New York, 2001.

[11]Mohite, P. M., "A generalized adaptive finite element modeling based analysis of undamaged and damaged laminated composite structures," Ph.D. Dissertation,Department of Aerospace Engineering, Indian Institute of Technology Kanpur India, 2006.

[12]Mohite, P. M., and Upadhyay, C. S. "Accurate computation of critical local quantities in composite laminate plates under transverse loading," *Computers and Structres*, Vol. 84, 2006, pp. 657, 675.

[13]Mohite, P. M., and Upadhyay, C. S., "A novel subdomainwise modeling approach for analysis of layered composite structures," *Proceedings of* 48^{th} *AIAA/ ASME/ ASCE/ AHS/ ASC Structures, Structural Dynamics and Materials Conference 1*, Newport, Rhode Island, 2006.

[14]Actis, R. L., Szabó, B. A., and Schwab, C., "Hierarchic models for laminated plates and shells," *Computer Methods in Appllied Mechanics and Engineering*, Vol. 172, 1999, pp. 79, 107.

[15]Gilat, A., Goldberg, R. K., and Roberts, G. D., "Strain rate sensitivity of epoxy resin in tensile and shear loading," NASA TM-213595, 2005.

[16]http://www.hexcel.com/NR/rdonlyres/901CD106-05F7-4133-A3F1-D4823DB31BD1/0/HexPly_M18_us.pdf

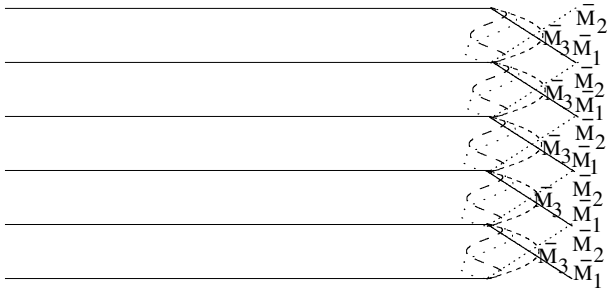

Figure 1. Director functions over layerwise model

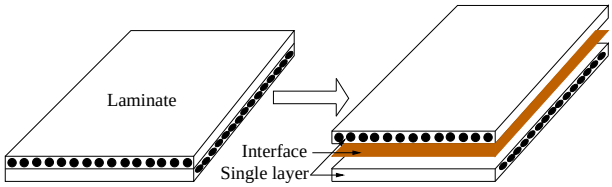

Figure 2. Mesomodel constituents in laminated composites

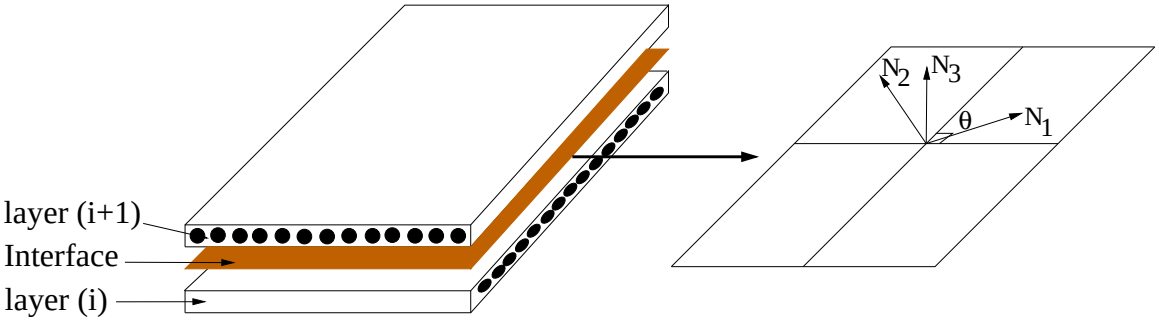

Figure 3. Orthotropic direction in interface

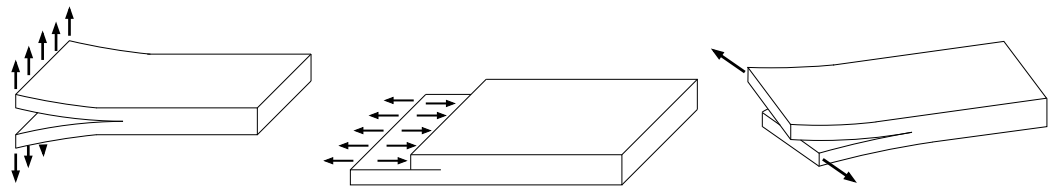

Figure 4. Interlaminar fracture modes

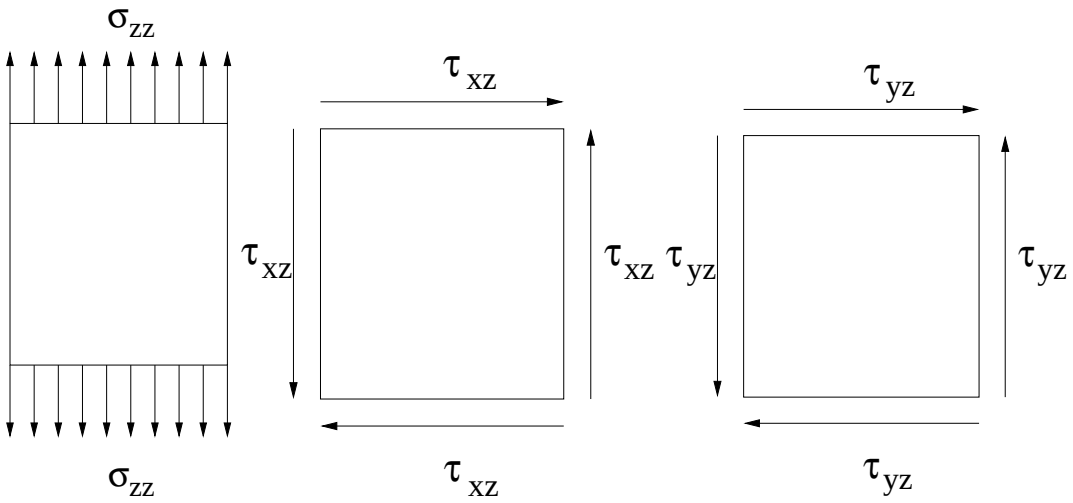

Figure 5. Transverse stress loading

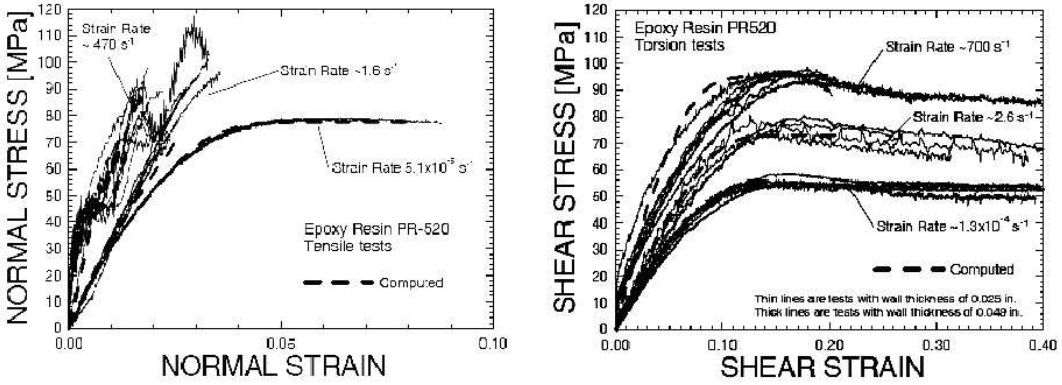

Figure 6. Stress strain curves at different strain rates for $PR-520$ epoxy[15]

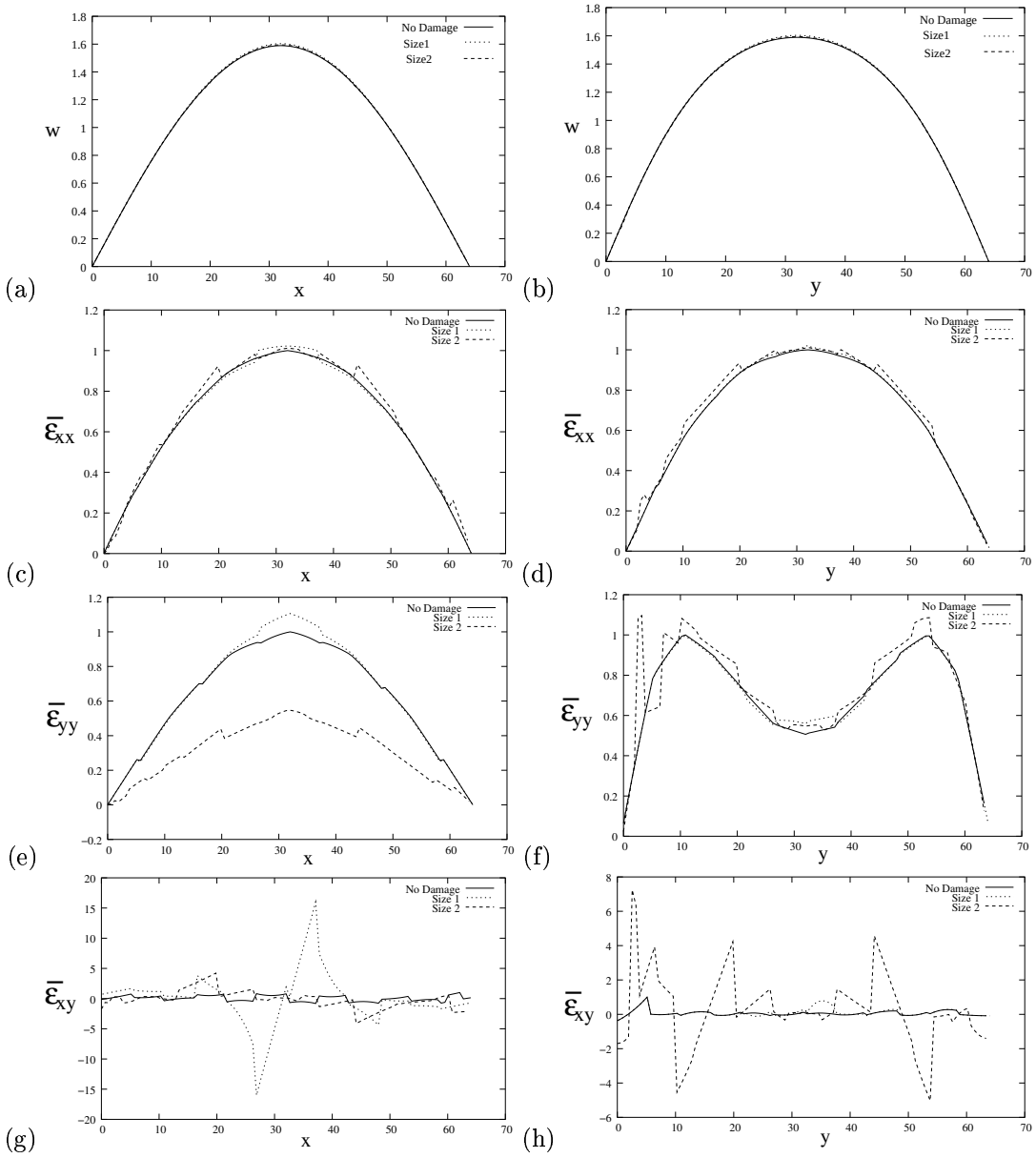

Figure 7. Transverse displacement and strains on top face of $[0/90/0]$ laminate due to damage of intensity $(0.1, 0.1, 0.98)$ in bottom ply

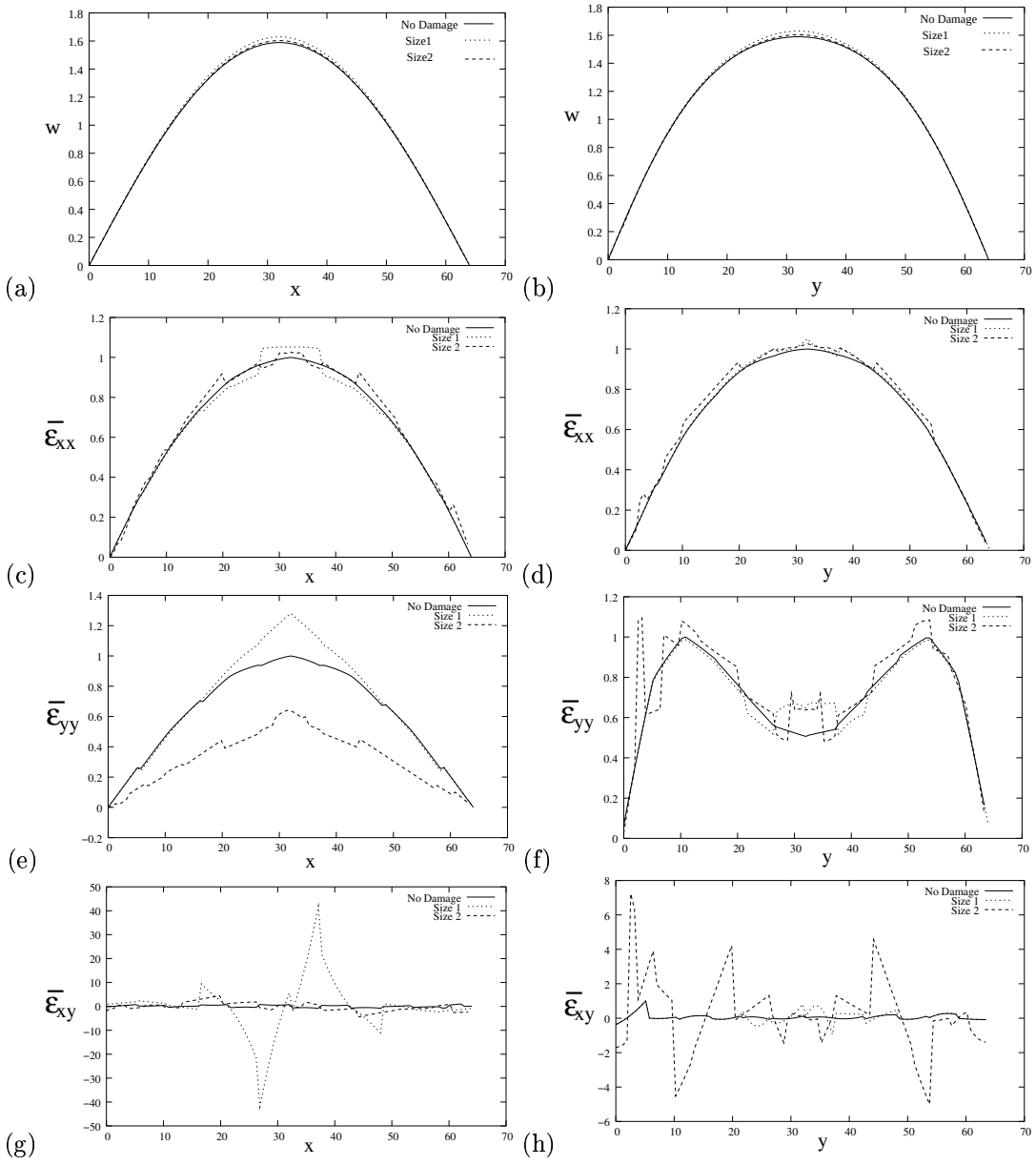

Figure 8. Transverse displacement and strains on top face of $[0/90/0]$ laminate due to damage of intensity $(0.1, 0.98, 0.1)$ in bottom ply

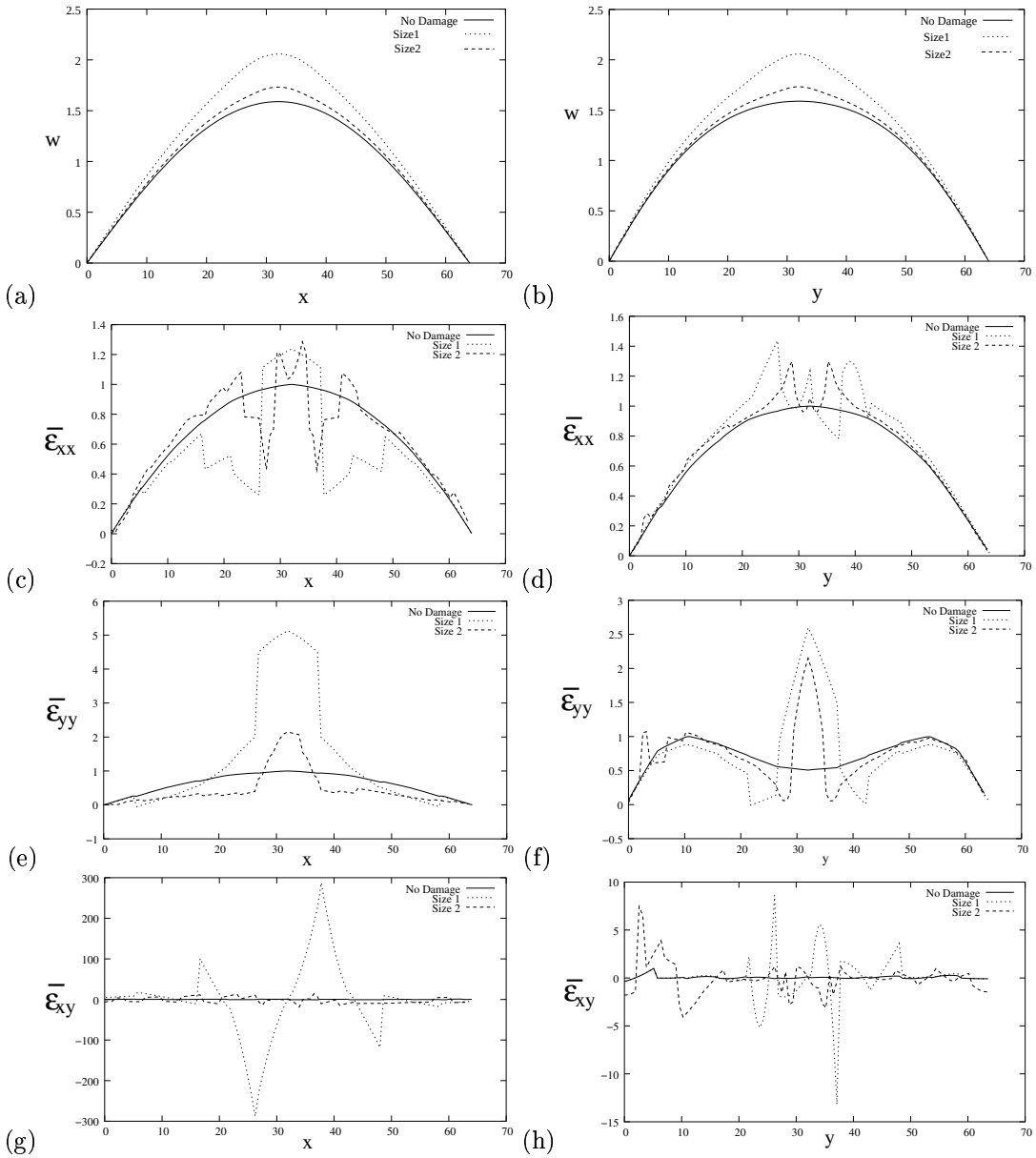

Figure 9. Transverse displacement and strains on top face of $[0/90/0]$ laminate due to damage of intensity $(0.98, 0.1, 0.1)$ in bottom ply

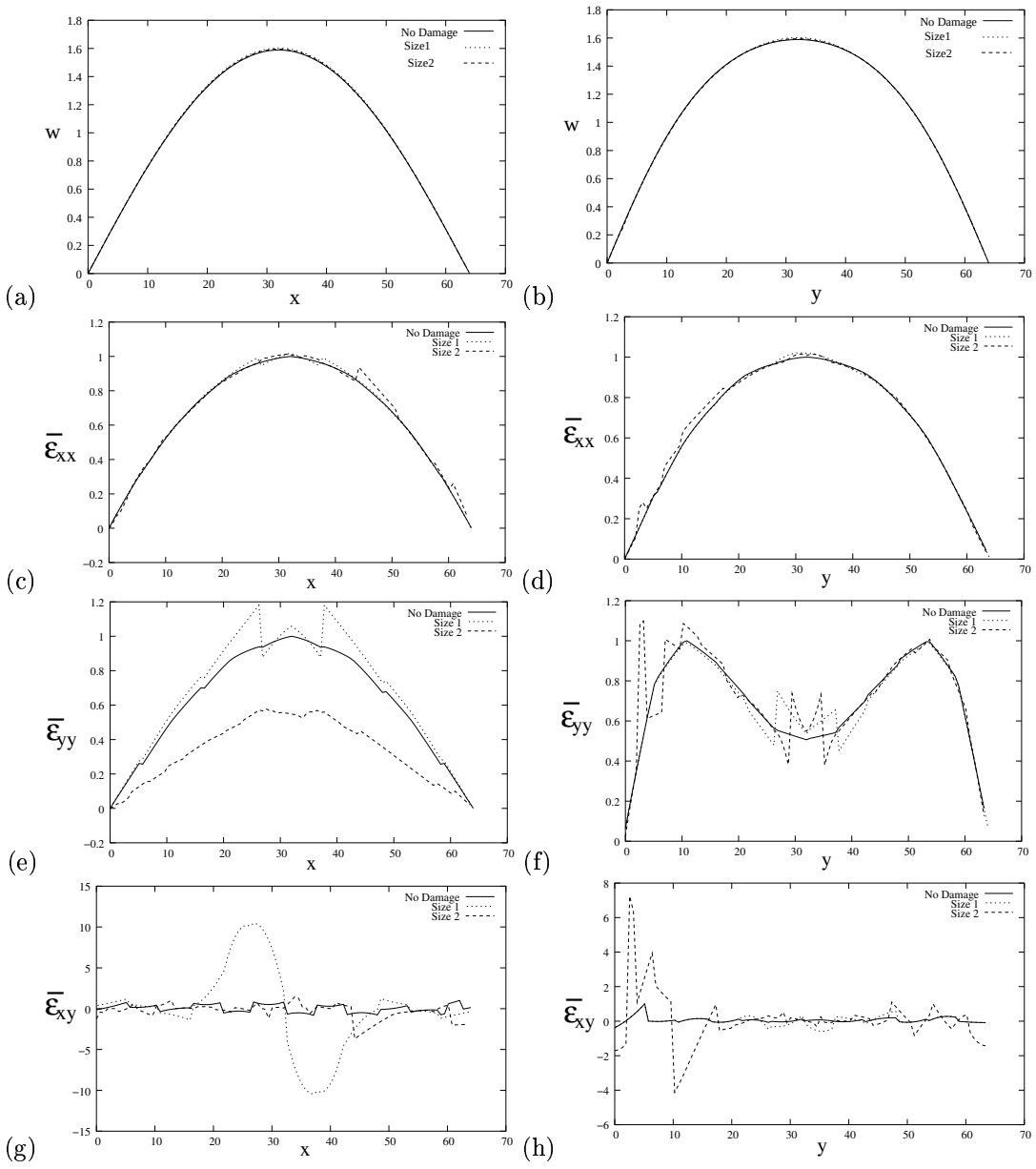

Figure 10. Transverse displacement and strains on top face of $[0/90/0]$ laminate due to damage of intensity $(0.98, 0.1, 0.1)$ in middle ply

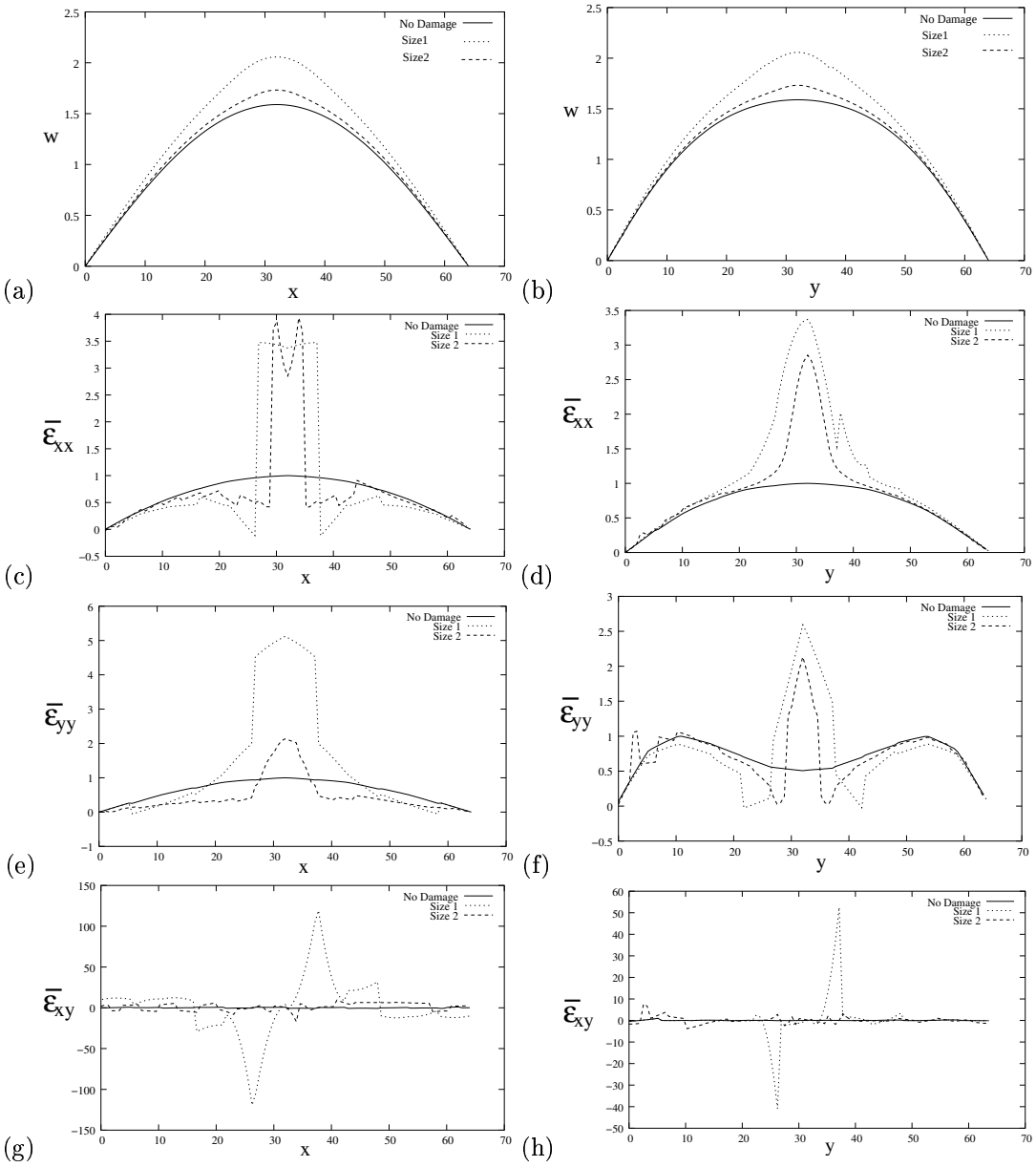

Figure 11. Transverse displacement and strains on top face of $[0/90/0]$ laminate due to damage of intensity $(0.98, 0.1, 0.1)$ in top ply

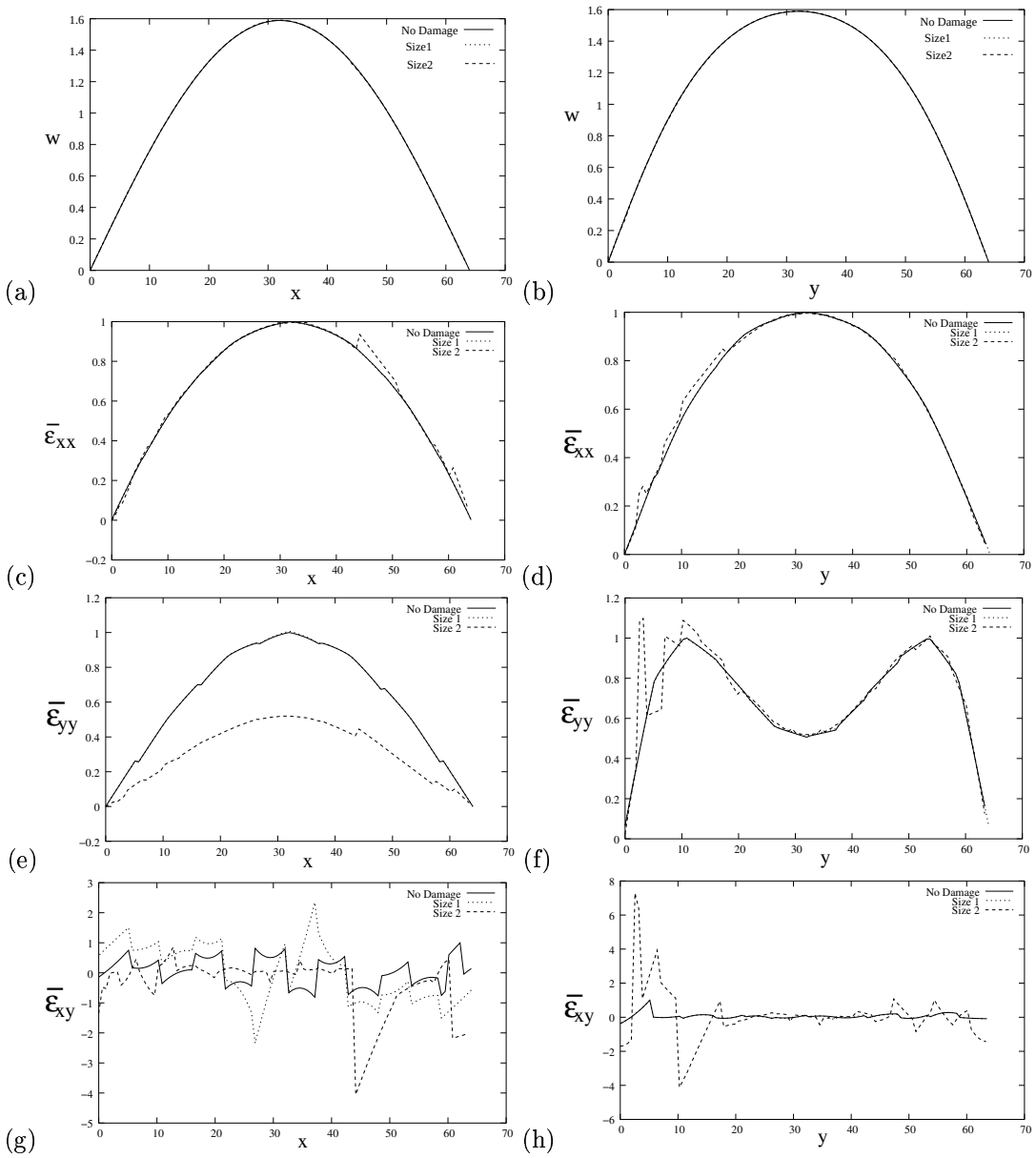

Figure 12. Transverse displacement and strains on top face of $[0/90/0]$ laminate due to damage of intensity $(0.98, 0.1, 0.1)$ in bottom $0/90$ interface

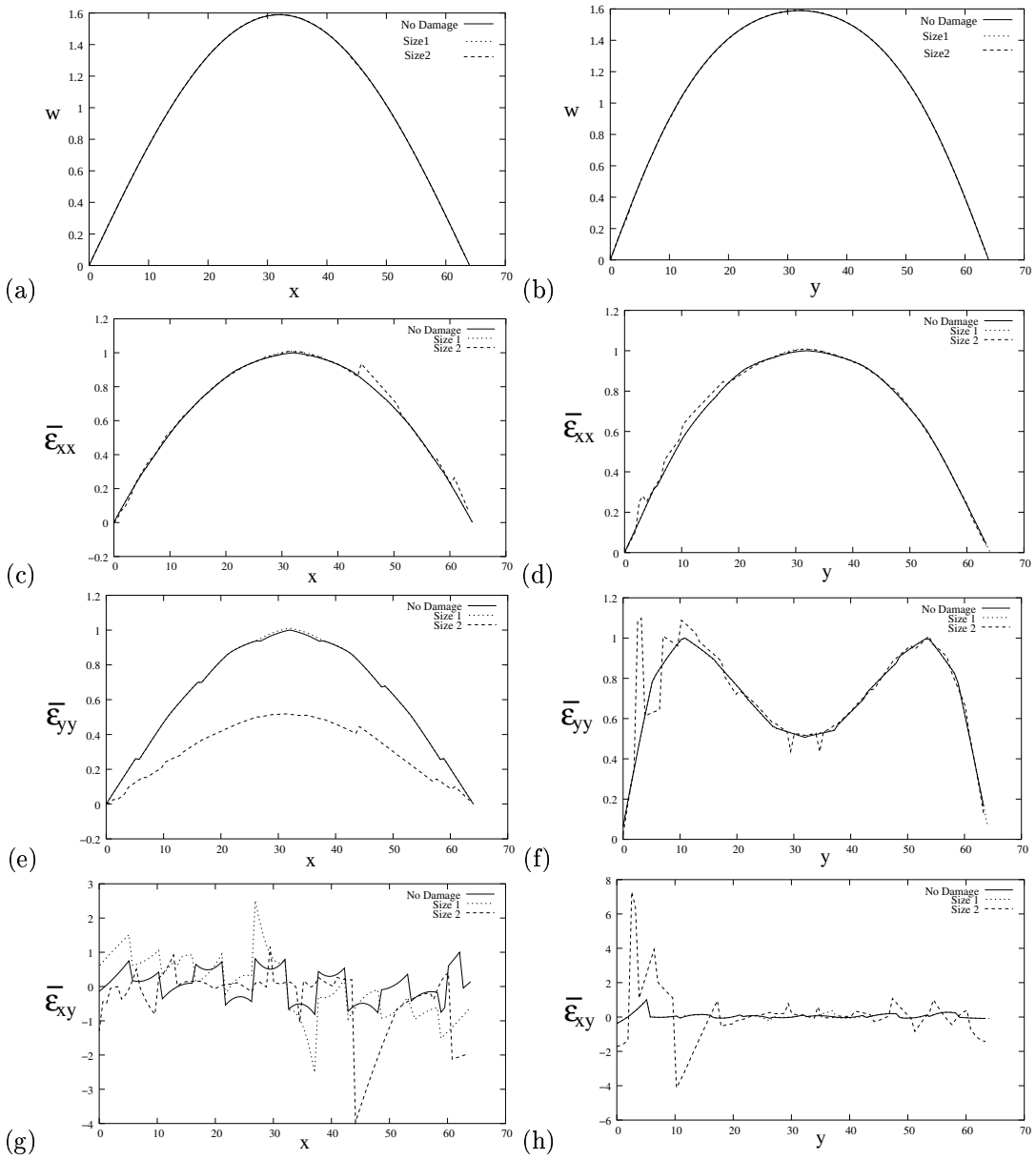

Figure 13. Transverse displacement and strains on top face of $[0/90/0]$ laminate due to damage of intensity $(0.98, 0.1, 0.1)$ in top $0/90$ interface

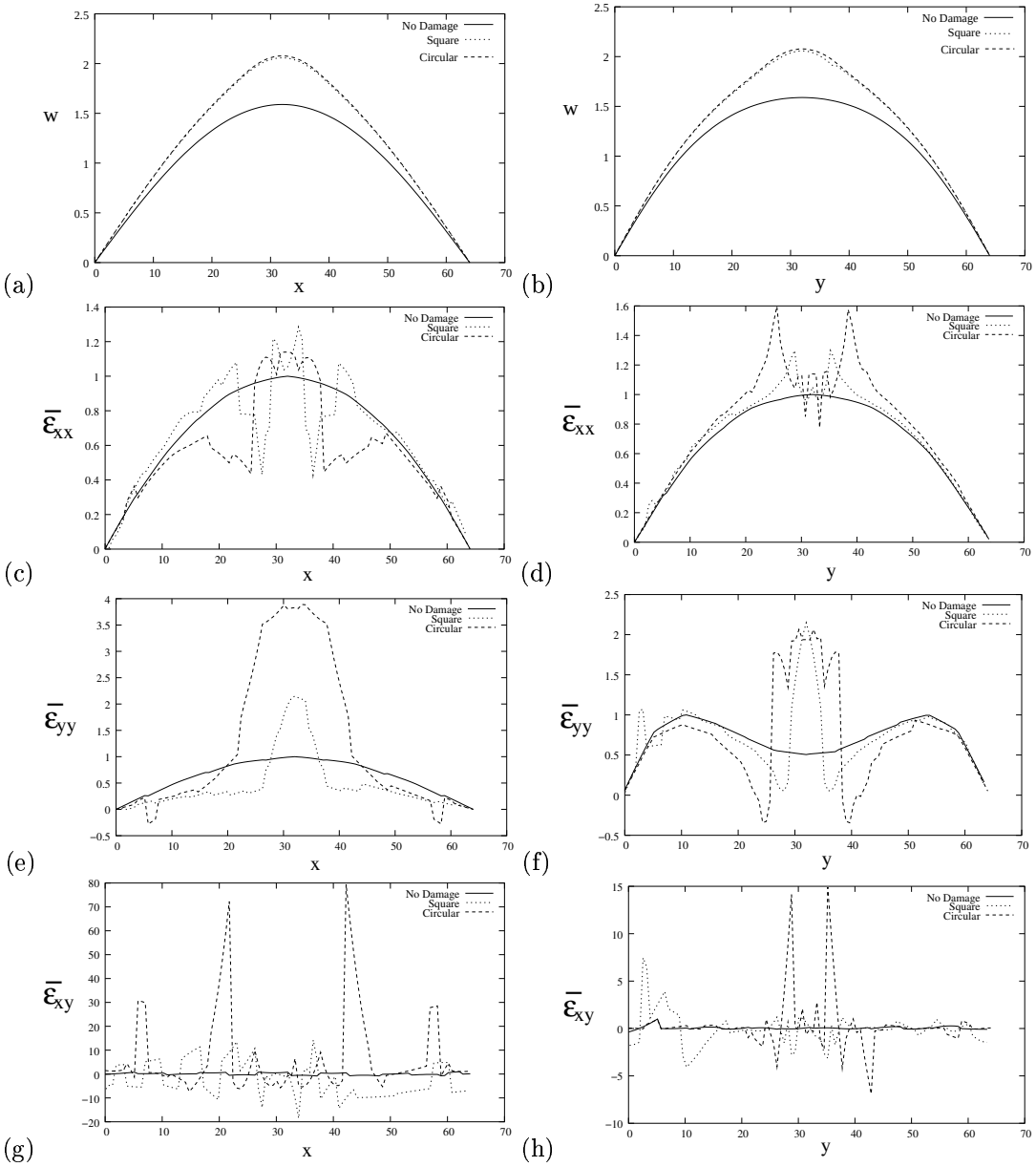

Figure 14. Transverse displacement and strains on top face of $[0/90/0]$ laminate due to damage of square and circular shape with same area and intensity $(0.98, 0.1, 0.1)$ in bottom ply

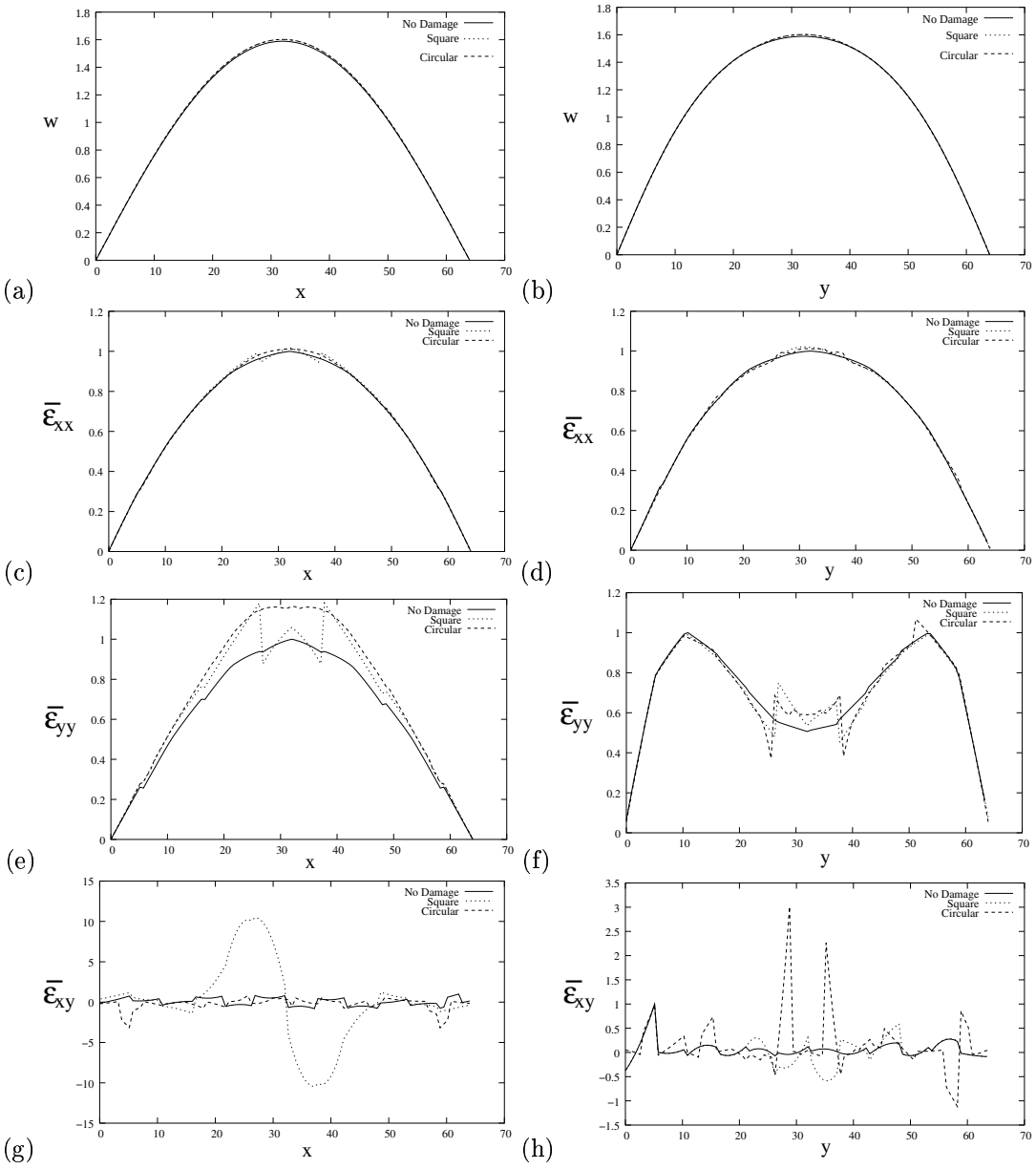

Figure 15. Transverse displacement and strains on top face of $[0/90/0]$ laminate due to damage of square and circular shape with same area and intensity $(0.98, 0.1, 0.1)$ in middle ply

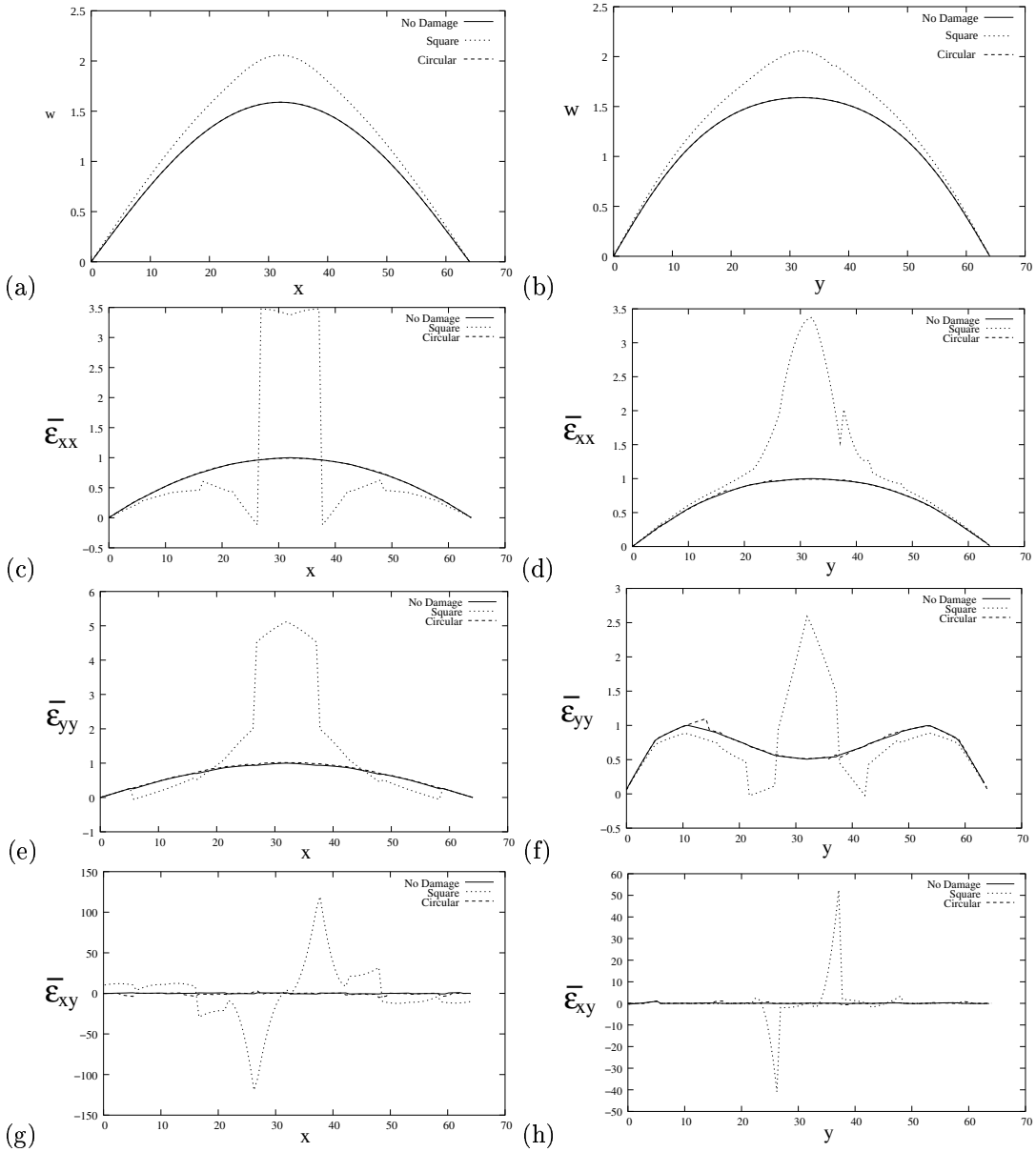

Figure 16. Transverse displacement and strains on top face of $[0/90/0]$ laminate due to damage of square and circular shape with same area and intensity $(0.98, 0.1, 0.1)$ in top ply

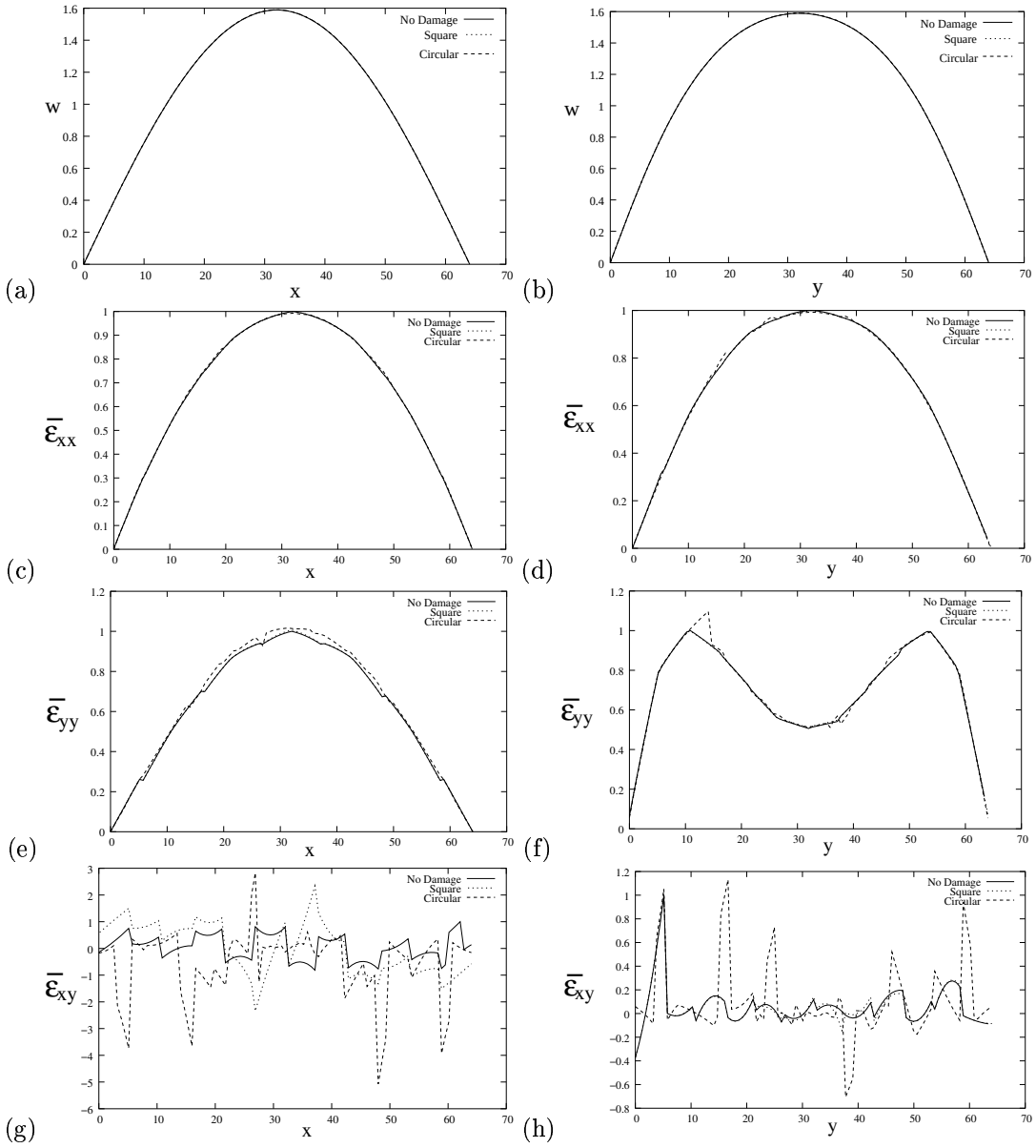

Figure 17. Transverse displacement and strains on top face of $[0/90/0]$ laminate due to damage of square and circular shape with same area and intensity $(0.98, 0.1, 0.1)$ in bottom $0/90$ interface

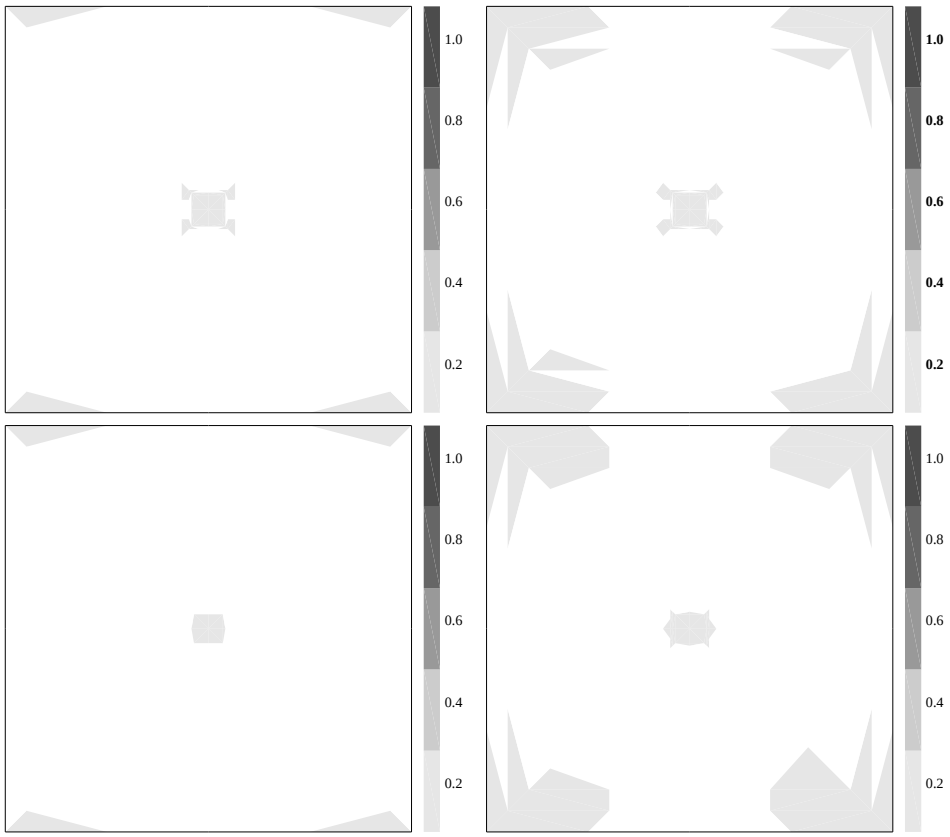

Figure 18. Damage initiation in other plies at different locations due to damage of size 2 and intensity $(0.98, 0.1, 0.1)$ **in bottom ply**

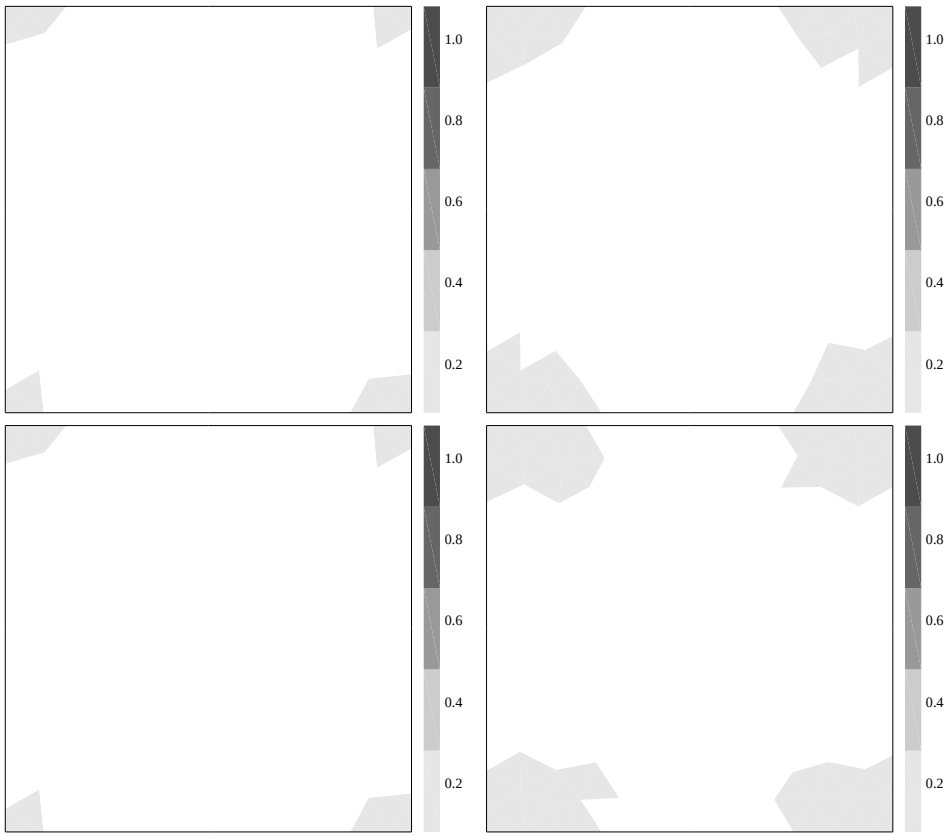

Figure 19. Damage initiation in other plies at different locations due to damage of circular shape with intensity $(0.98, 0.1, 0.1)$ **in bottom** $0/90$ **interface**

Table 1. Material properties for $M55J/M18$ Graphite/Epoxy composite[8]

Property	E_{11}	$E_{22} = E_{33}$	$G_{12} = G_{13} = G_{23}$	$\nu_{12} = \nu_{13} = \nu_{23}$	t_i
Value	$280\,GPa$	$6.0\,GPa$	$4.8\,GPa$	0.3	$0.1\,mm$

Table 2. Material properties for M18 Epoxy[16]

Property	$E_{11} = E_{22} = E_{33}$	$G_{12} = G_{13} = G_{23}$	$\nu_{12} = \nu_{13} = \nu_{23}$
Value	$3500\,MPa$	$1268.2\,MPa$	0.38

Table 3. Damage parameters for ply and interface for $M55J/M18$ Graphite/Epoxy composite[8]

Damage parameters for ply

Parameter	Y_d^0	Y_d^c	$Y_{d'}^0$	$Y_{d'}^c$	Y_r	ε_F^R
Value	$0.0016\,MPa$	$29.38\,MPa$	$0.003\,MPa$	$16.16\,MPa$	$0.16\,MPa$	1.51%

Damage parameters for interface

Parameter / Interface	Y_c (N/mm)	λ_1, λ_2	α
[0/0]	0.113 ± 0.007	0.37 ± 0.07	2.0 ± 0.3
[±22.5]	0.167 ± 0.013	0.36 ± 0.07	1.4 ± 0.3
[±45]	0.192 ± 0.014	0.33 ± 0.05	1.2 ± 0.1